Journal of Applied Polymer Science

Fabrication and Properties of Carbon Nanotube/Styrene–Ethylene–Butylene–Styrene Composites via a Sequential Process of (Electrostatic Adsorption Aided Dispersion)-Plus-(Melt Mixing)

Zhaofeng Wu, Hua Wang, Xingyou Tian, Xin Ding, Haifeng Zhou, Xianzhu Ye

Key Laboratory of Materials Physics, Institute of Solid State Physics, Chinese Academy of Sciences, Hefei 230031, People's Republic of China

Correspondence to: X. Tian (E-mail: xytian@issp.ac.cn)

ABSTRACT: Carbon nanotube (CNT)/styrene–ethylene–butylene–styrene (SEBS) composites were prepared via a sequential process of (electrostatic adsorption assisted dispersion)-plus-(melt mixing). It was found that CNTs were uniformly embedded in SEBS matrix and a low percolation threshold was achieved at the CNT concentration of 0.186 vol %. According to thermal gravimetric analysis, the temperatures of 20% and 50% weight loss were improved from 316°C and 352°C of pure SEBS to 439°C and 463°C of the 3 wt % CNT/SEBS composites, respectively. Meanwhile, the tensile strength and elastic modulus were improved by about 75% and 181.2% from 24 and 1.6 MPa of pure SEBS to 42 and 4.5 MPa of the 3 wt % CNT/SEBS composite based on the tensile tests, respectively. Importantly, this simple and low-cost method shows the potential for the preparation of CNT/polymer composite materials with enhanced electrical, mechanical properties, and thermal stability for industrial applications. © 2013 Wiley Periodicals, Inc. J. Appl. Polym. Sci. **2014**, *131*, 40227.

KEYWORDS: composites; mechanical properties; applications; thermogravimetric analysis (TGA)

Received 11 September 2013; accepted 24 November 2013
DOI: 10.1002/app.40227

INTRODUCTION

As carbon nanotubes (CNTs) were discovered in 1991, the extremely high modulus, strength, excellent electrical and thermal conductivity enable them for a wide range of applications.[1,2] One of the most intriguing applications of CNTs is the CNT/polymer composites with enhanced mechanical and electrical properties.[3–5] In order to achieve enhanced electrical and mechanical properties, CNTs need to be well dispersed in polymer matrix. Currently, the chemical modifications of CNTs have been intensively studied as an efficient approach to increase their dispersion in polymer matrix. However, the modified CNTs are often accompanied by the sacrifice of electrical property of the composites.[6,7] In addition, these methods are usually complex, time consuming, requiring large quantity of solvents and unsuitable for large-scale fabrication.[8] Melt mixing has been the most promising approach for the production of CNT/polymer composites on industrial scale because of its speed, simplicity, and easy integration into standard industrial facilities, particularly for thermoplastic polymers.[9,10] For polar thermoplastics with functional groups, the high polarity similarity between basal resin and CNTs[11] and/or the additional physical bonding arisen from a combination of shear stress and thermal activation[12] could induce relatively good dispersion of CNTs. Nevertheless, for nonpolar ones, such as polyolefin and styrene–ethylene–butylene–styrene (SEBS), there present a challenge to achieve the fine dispersion of CNTs merely by melt mixing.[13,14]

Subsequently, the solvent-assisted predispersion of CNTs in polymer particles under ultrasonication, followed by melt mixing, improved the dispersion of CNTs in the CNT/polymer composites.[13,15,16] Lu et al.[17] developed a so-called latex technology that isotactic polypropylene (iPP) latex was mixed into aqueous CNT suspended solution containing commercial surfactant likes sodium dodecyl sulfate, after evaporation of liquid components a filamentous dispersion of CNTs could be achieved. Similarly, SEBS particles and CNTs were dispersed in the mixed solution of alcohol and liquid bisphenol A bis(diphenyl phosphate), a halogen-free flame retardant, by ultrasonic dispersion and stirring.[16] After evaporation of alcohol, the SEBS particles coated uniformly by CNTs with bisphenol A bis(diphenyl phosphate) as the adhesive were obtained. The predispersion state, in which the SEBS particles were coated uniformly by CNTs, improved the dispersion of CNTs during the subsequential process of melt mixing, accounting for the enhanced mechanical and flame-retardant properties. Although the physical methods mentioned above improved effectively the

dispersion of CNTs, they still required a great liquid chemical solvent, time, and electrical energy.[14]

To avoid this problem, a simple and effective method to realize excellent comprehensive performances in iPP/multi-walled CNTs (MWCNTs) was developed.[14] Before melt extrusion, solid-state iPP powders and MWCNTs were premixed by high-speed rotating. By this way, the dispersion of MWCNTs was significantly improved compared with the common one-step melt extrusion strategy. The fine dispersion of MWCNTs was mainly contributed to the static electric attraction yielded by friction between iPP granules and MWNCTs and the more surfaces of the broken iPP granule.[14] It is well known that static charges accumulate easily on insulating surfaces, especially for the non-polar polymer powders.[18] Therefore, static charges can be exploited in terms of electrostatic adsorption to improve the dispersion of CNTs.

Based on the above discussion, the electrical, mechanical performances, and thermal stability of the MWCNT/SEBS composites prepared via the sequential process of (electrostatic adsorption assisted dispersion)-plus-(melt mixing) (EAMM) were investigated.

EXPERIMENTAL

Materials

SEBS (Kraton G 1652) with a molecular weight Mw = 57,000, a styrene/butadiene ratio (w/w) = 30/70, was supplied by Shell Chemical, USA. MWCNTs (Chengdu Institute of Organic Chemistry, China), with purity: >95%, length: 10–30 μm, diameter: 10–20 nm, special surface area: > 200 m^2/g, electrical conductivity: >100 S/cm, were used in this study. MWCNTs were used as-received without any chemical treatments.

Sample Preparation

Electrostatic charges occur whenever two surfaces are separated, where at least one of them is highly electrically insulating.[18] When SEBS powders are sifted, the large particles are broken into small particles and both the sieve and SEBS particles will be charged, as shown in Figure 1. In addition, electrostatic charges can also be generated by rubbing between brushes and SEBS particles.[19] In our work, after drying of SEBS particles and MWCNTs for 4 h at 70°C, they were sifted using 20- and 100-mesh sieves, respectively. In the process of sifting, the non-polar SEBS particles produced static charges because of the rubbing between brushes and particles, and the separation of particles (Figure 1). After mixing of SEBS particles with electrostatic charges and MWCNTs by stirring for 3 min, the efficient dispersion of MWCNTs on the surfaces of SEBS particles with the help of electrostatic adsorption was achieved. Then the pre-dispersed MWCNT/SEBS hybrid was mixed by a XSS-300 torque rheometer (Shanghai Kechuang Rubber Plastic Mechanical Equipment), and the screw speed, mixing time, and mixing temperature were set to 100 rpm, 8 min, and 190°C, respectively. In addition, another group of MWCNT/SEBS composites were prepared by the conventional melt mixing using the same parameters. The densities (ρ) of the SEBS, MWCNTs in this study are about 0.91 and 2.1 g/cm^3, respectively. The volume

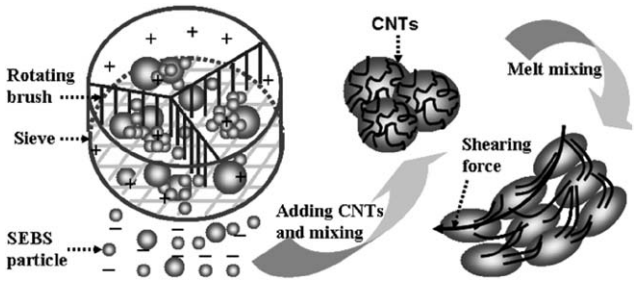

Figure 1. Creation of electrostatic charges and the preparation of composites.

fraction of MWCNTs can be calculated based on the densities of the constituents:

$$V_{CNT} = \frac{W_{CNT}/\rho_{CNT}}{W_{CNT}/\rho_{CNT} + W_M/\rho_M}$$

where W represents the weight and subscript M denotes the polymer matrix.

Characterization

The electrical conductivity was measured using a digital, four-point probe RTS-9 resistivity measurement system at room temperature, and the diameter and thickness of the specimens are 11.48 and 2–2.5 mm, respectively. High resistivity meter LK2679A was used to measure the volume resistivity of specimens (100 × 13 × 3 mm^3) with high volume resistivity beyond 10^6 Ω cm and silver paste was coated on the surface of the specimens to ensure good contact of the specimens with the electrodes. The conductivity data were from an average of five measurements. The morphology of samples was observed under a sirion-200 (FEI, America) scanning electron microscopy (SEM) with an accelerating voltage of 10 kV. Transmission emission microscopy (JEM-2010 TEM) was used to observe the morphology of CNTs. Thermal gravimetric analysis (TGA) was carried out by a Q5000 IR thermal gravimetric analyzer at a heating rate of 10°C/min under air conditions. All the samples were kept at 5–10 mg in an open alumina pan and tested from room temperature to 700°C. The tensile tests were carried out using an instron universal material testing system (model 5567) at room temperature with gauge length of 25 mm and cross-head speed of 100 mm/min. Values of mechanical property reported here represented an average of the results for three tests. Dynamic viscoelastic behaviors of samples with size of 40 × 6 × 1 mm^3 were investigated using a dynamic mechanical analyzer (Pyris Diamond DMA) with a heating rate of 2°C/min.

RESULTS AND DISCUSSION

Tensile Property and Reinforcement Mechanisms

The morphology of SEBS particles coated uniformly by CNTs with the help of electrostatic adsorption is shown in Figure 2(a,b). From the enlarged morphology of selected region (the inset) in Figure 2(a), CNTs are uniformly dispersed on the surfaces of SEBS particles with the help of electrostatic adsorption. Figure 2(c,d) shows the fine dispersion of CNTs in the 1.5 wt % CNT/SEBS mixed at 190°C for 3 min before compression molding. Clearly, SEBS particles become small because of the shearing of rotors and intense friction among SEBS particles.[16]

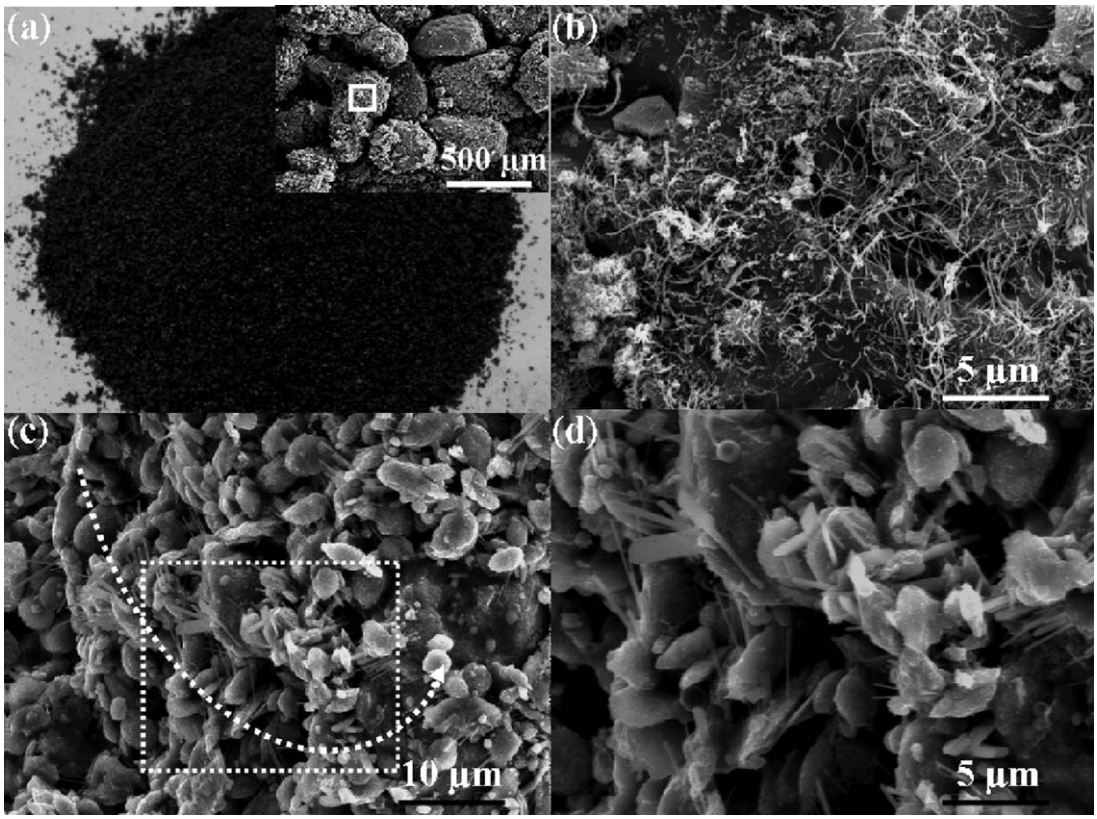

Figure 2. (a) Photo and SEM image (the inset) of SEBS particles coated by 2 wt % CNTs; SEM images; (b) enlarged morphology of selected region in (a); (c) 2 wt % CNT/SEBS mixed for 3 min before compression molding, (the dotted arrow represents the direction of friction or shearing forces); and (d) enlarged morphology of selected region in (c).

Although the SEBS matrix is still in a particulate state because of the incomplete melting, CNTs or their bundles are uniformly embedded in SEBS particles in a filamentous stretched state, as shown by the dotted arrow in Figure 2(c).

The filamentous stretched CNTs and their bundles could be illustrated by Figure 1. In the process of melt mixing, the polymer particles were in a semimolten state at the beginning stage and their tensile strength and elastic modulus was weakened greatly because of the high temperature. As shown by the solid arrow in Figure 1, the semimolten polymer particles were stretched by strong shearing forces of the rotors and intense friction among the SEBS particles, merging new particles, or broken into smaller particles, which was consistent with Figure 2(c). Simultaneously, CNTs adsorbed on the surfaces of polymer particles were stretched and embedded in smaller particles along with the stretched SEBS matrix and the fracture of SEBS particles. As a result, the stretched CNTs bridged across the broken smaller polymer particles as shown in Figure 2(c,d).

Uniform dispersion of CNTs in CNT/SEBS composites was also displayed by the SEM and TEM images in Figure 3. As shown by the fractured surfaces of the (0.21 vol %) 0.5 wt % CNT/SEBS and (0.87 vol %) 2 wt % CNT/SEBS [Figure 3(a,c)], CNTs were also uniformly and tightly embedded in SEBS matrix, which indicated that the uniform predispersion of CNTs was preserved and improved during the subsequential process of melt mixing. As shown by TEM images [Figure 3(b,d)], CNTs were in a state of filamentous dispersion in SEBS matrix, and no obvious aggregation was found at 2 wt % CNTs. The uniformly dispersed CNTs in the 0.5 wt % CNT/SEBS showed the formation the conductive network at the 0.21 vol % CNT content, which was insistent with the percolation threshold discussed later. Clearly, most CNTs were separated into filamentous tubes or bundles in SEBS matrix via the sequential process of EAMM, which was very important to the high electrical and mechanical performances. By contrast, the conventional melt mixing usually makes the CNTs randomly distribute in composites, thus a large number of CNTs are needed to form conductive networks. As indicated by Figure 3(e,f), CNTs exist in the form of agglomeration in the 2 wt % CNT/SEBS prepared by the conventional melt mixing. The obvious contrast of CNT dispersion in SEBS matrix indicates that the EAMM method effectively improves the dispersion of CNTs compared with the conventional melt mixing.

Mechanical properties of pure SEBS and CNT/SEBS composites with different CNT contents were shown in Table I. It can be seen that the tensile strength of the CNT/SEBS composites significantly increased with the increasing CNT content. After introduction of only 1, 2, and 3 wt % CNTs into SEBS matrix, the tensile strength was greatly improved by about 29%, 58%, and 75% from 24 MPa of pure SEBS to 31, 38, and 42 MPa, respectively. Meanwhile, their elastic modulus was improved by about 62.5%, 143.7% and 181.2% from 1.6 MPa of pure SEBS

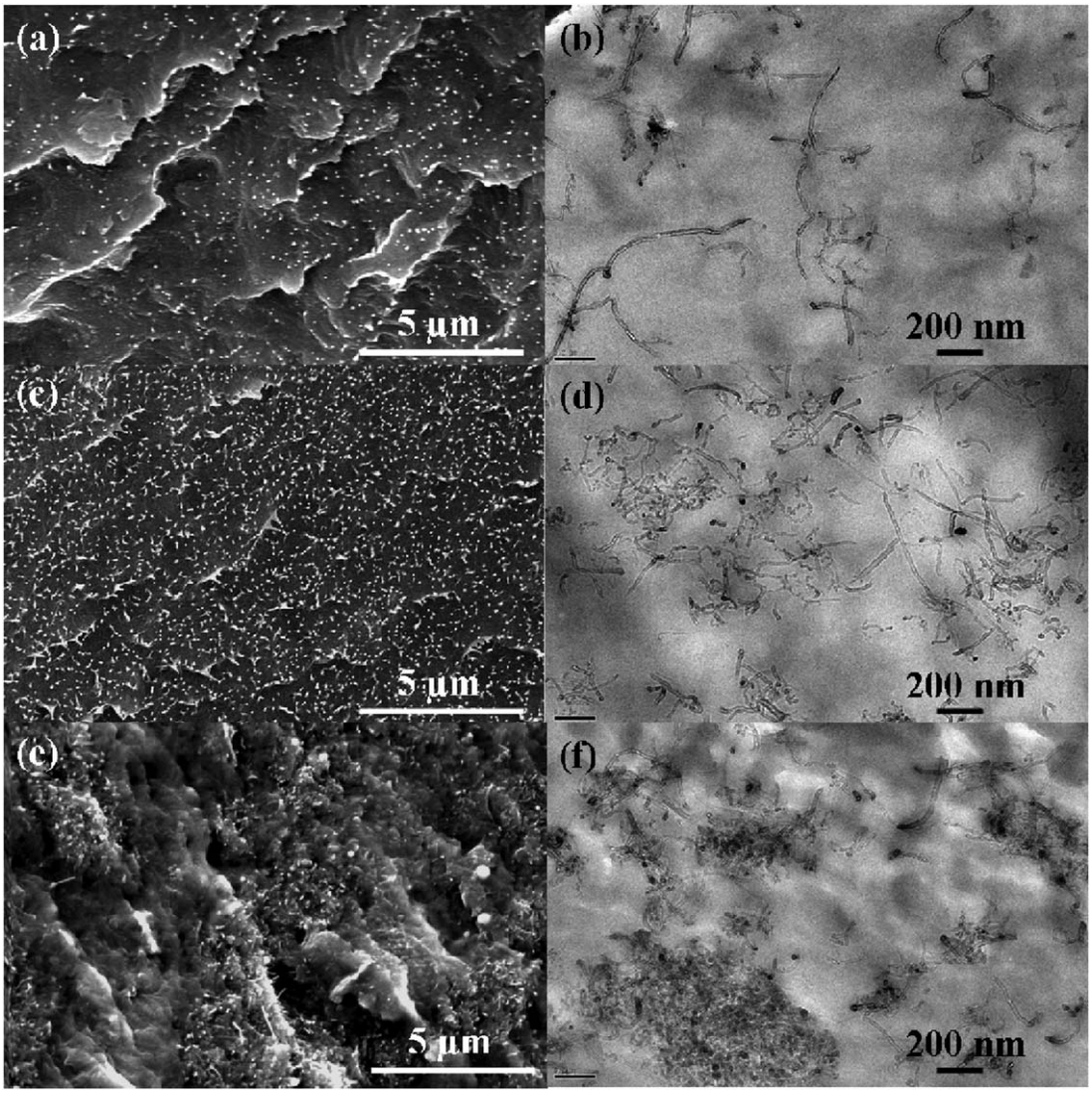

Figure 3. (a), (c) and (b), (d) represent SEM and TEM images of (0.21 vol %) 0.5 wt % and (0.87 vol %) 2 wt % CNT/SEBS composites prepared by the EAMM method, respectively; (e) SEM image and (f) TEM image of 2 wt % CNT/SEBS composites prepared by the conventional melt mixing.

to 2.6, 3.9 and 4.5 MPa, respectively. Compared with the pure SEBS, the decreasing elongation at break indicated that 2 wt % CNT/SEBS and 3 wt % CNT/SEBS composites became somewhat brittle. Nevertheless, the slight improvement in the elongation at break for composites with 0.5–1.0 wt % CNTs was also displayed in Table I. The possible strengthening and toughening mechanisms will be discussed later by SEM observations.

Figure 4 shows a typical overview on the fractured surface of the 1 wt % CNT/SEBS. It can be seen that the CNTs are not entirely pulled out but fully stretched during the deformation and failure processes. Most stretched CNTs or their bundles are well aligned, clearly indicating that stretching can align CNTs or their bundles, as observed by other researchers.[20,21] And, the well-aligned CNTs and their bundles bridge across the cracks or holes, which allows the release of stress, absorbs the fracture energy[21] diverts, even terminates the evolution of cracks or holes, thus contributing to toughness improvement.[16]

Moreover, closer inspection indicates that upon failure almost all of the CNTs are in a filamentous stretched state, while a few are broken apart but not pulled out [Figure 4(b)]. The CNTs, as indicated by the solid arrows in Figure 4(a), are observed to be broken,

Table I. Mechanical Properties of Pure SEBS and CNT/SEBS Composites with Different CNT Content

CNT content (wt %)	Elastic modulus (MPa)	Tensile strength (MPa)	Elongation at Break (%)
0	1.6 ± 0.1	24 ± 1.2	818 ± 25
0.5	2.1 ± 0.1	28 ± 1.8	830 ± 30
1.0	2.6 ± 0.2	31 ± 2.1	825 ± 25
1.5	3.2 ± 0.2	34 ± 1.8	772 ± 30
2	3.9 ± 0.3	38 ± 2.5	718 ± 25
3	4.5 ± 0.3	42 ± 3.5	672 ± 30

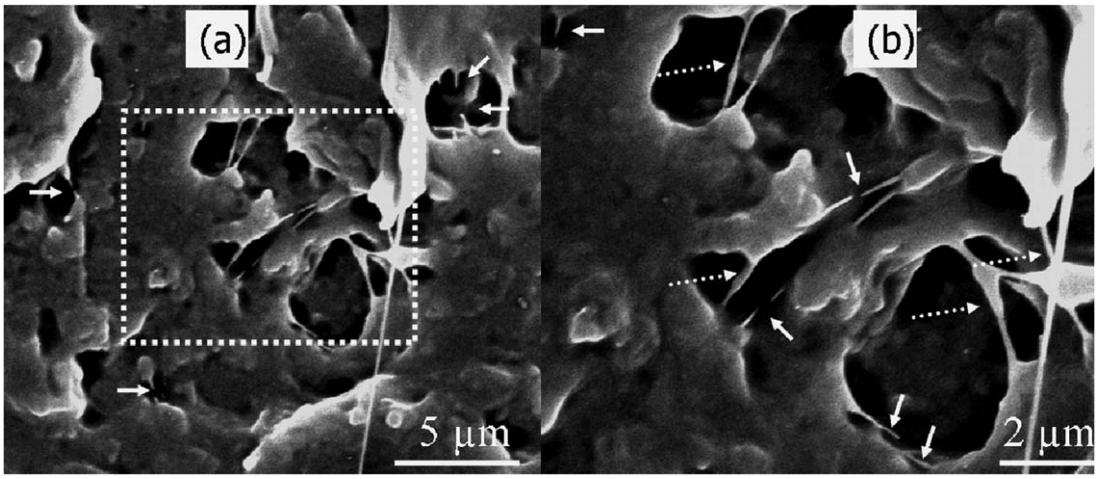

Figure 4. (a) SEM images showing micro cracks linked by stretched CNTs and their bundles in 1 wt % CNT/SEBS after the stress-strain test. (b) Enlarged morphology of selected region in (a).

while the other two ends still strongly embed in the matrix. This typical breakage phenomenon of the CNTs upon tensile stretching indicates a strong interfacial adhesion between CNTs and polymer matrix and an effective load transfer from the polymer matrix to CNTs.[21] Interestingly, a bead- or ball-like morphology along the stretched CNTs or their bundles is observed under close inspection at higher magnification, as indicated by the dotted arrows in Figure 4(b). It is reasonably believed that these beads are the absorbed polymer protruding or layers around CNTs, showing the intimate contact and good adherence of polymer matrix to the CNTs.[21–23] It is thus believed that the strong interfacial adhesion observed above is responsible for the enhanced mechanical property shown in Table I.

In addition, belt-like CNTs are observed which interconnect two polymer lumps, as shown by the dotted arrows in Figure 4(b). Obviously, this interconnection is realized by single CNT or their bundles wrapped by the matrix as its diameter is much bigger than other broken tubes observed on the fracture surface.[23] Moreover, the middle part of the bundle is smaller than the two ends adhered to the polymeric lumps, also indicating the strong interconnection of CNTs and SEBS matrix.

Dynamic Viscoelastic Behaviors of the CNT/SEBS Composites

Figure 5 shows the dynamic mechanical property of pure SEBS and its composites. It can be seen that with the increasing CNT content the storage modulus of the composites increase gradually, especially in the range of −30 to 100°C [Figure 5(a)]. Compared with the pure SEBS (79 MPa), the storage modulus of 0.5 wt % CNT/SEBS (108 MPa), 1.5 wt % CNT/SEBS (164 MPa) and 3 wt % CNT/SEBS (396 MPa) exhibits 37%, 108% and 401% increment at 25°C, respectively. The significant improvement in storage modulus should be ascribed to the combined effect of the high performance and the good dispersion of CNTs with a high aspect ratio.[16,21]

SEBS block copolymer has the glass transition temperature (Tg) of the soft, ethylene/buthylene phase at −30°C and Tg of the hard, polystyrene phase at 110°C. The same values for those Tg were found in previous reports.[24] As displayed in Figure 5(b), both the Tg of soft blocks and the Tg of hard blocks remain almost unchanged after the introduction of CNTs into SEBS matrix, probably indicating that less constraints from one-dimensional CNT nanofiller are imposed on the polymer chains.[21] This is different from the case usually reported in

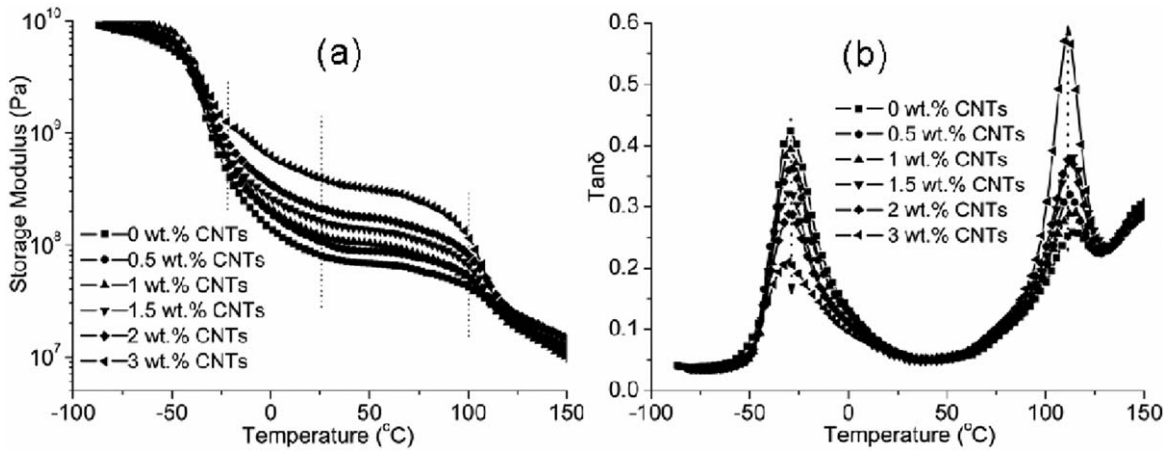

Figure 5. Temperature dependence of (a) storage modulus and (b) loss factor (tan δ) of pure SEBS and its composites at 5 Hz.

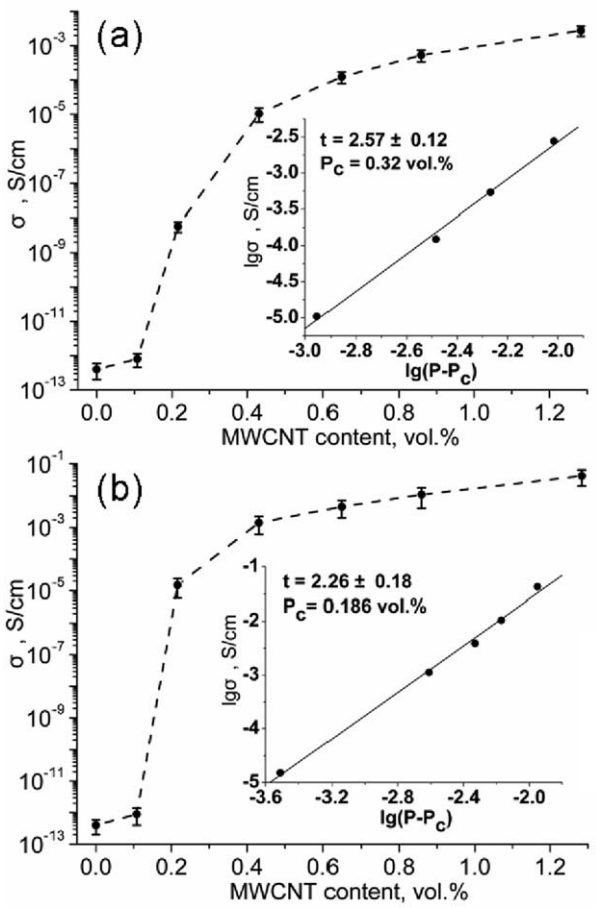

Figure 6. Relation of electrical conductivity and CNT content for CNT/SEBS composites prepared by (a) conventional melt mixing and (b) EAMM method. The insets show the percolation scaling law between log σ and log $(P-P_c)$ for $P > P_c$.

two-dimensional layered silicates reinforced polymer composites,[25] where the mobility of polymeric chains is greatly constricted by the confinement from two-dimensional nanoclays, thus usually increasing the Tg of the composites.[26,27]

In addition, all composites show the lowering of tan δ peaks of soft blocks (0.21 from 0.41) and the increase of tan δ peaks of hard blocks (0.56 from 0.25) with the increasing CNT content. A possible mechanism of this phenomenon is that the addition of CNTs altered the microphase separation behavior of SEBS, namely, the tendency of polystyrene phase coalescence is enhanced by CNTs. This phenomenon clearly indicates that CNTs are uniformly dispersed in SEBS matrix and have a strong interaction with SEBS matrix.[27] In summary, the mechanical properties of CNT/SEBS composites are improved significantly after the addition of CNTs, which should be attributed to the uniform dispersion of CNTs in SEBS matrix, phase separation of SEBS enhanced by CNTs and strong interfacial interaction between CNTs and SEBS matrix.

Percolation Threshold of the CNT/SEBS Composites

Figure 6 shows the relation of electrical conductivity and CNT content. The percolation thresholds are observed in the intervals of 0.2–0.4 vol % and 0.1–0.3 vol % for the CNT/SEBS prepared by conventional melt mixing and CNT/SEBS prepared by EAMM, respectively. At this stage, the conductivity is controlled by the conducting CNT networks. Percolation theory defines an insulator–conductor transition and a corresponding threshold of concentration (P_c) of the conductive filler, via the following equation[28]:

$$\sigma = \sigma_o (p - p_c)^t \quad for \; p > p_c \tag{1}$$

where σ_0 is a constant, p the volume fraction of conductive fillers, and t the critical exponent. As shown by the insets in Figure 6(a,b) for the lg σ versus lg$(p - p_c)$ plot, the conductivity of the CNT/SEBS prepared by conventional melt mixing and CNT/SEBS prepared by the EAMM method agrees with the percolation behavior predicted by eq. (1). For the CNT/SEBS prepared by conventional melt mixing, the fitted straight line in Figure 6(a) with $P_c = 0.32$ vol %, and $t = 2.57 \pm 0.12$ gives a good fit to the data. The value of the critical exponent, t is found to be close to the universal value to three-dimensional percolating systems.[29–31] For the CNT/SEBS prepared by the EAMM method, the fitted straight line in Figure 6(b) with $P_c = 0.186$ vol % and $t = 2.27 \pm 0.18$ also gives an excellent fit to the data. The low percolation threshold indicates the efficient dispersion of CNTs in SEBS matrix at low concentration, which is confirmed by Figure 3(b). The obvious difference in percolation thresholds of the CNT/SEBS prepared by conventional melt

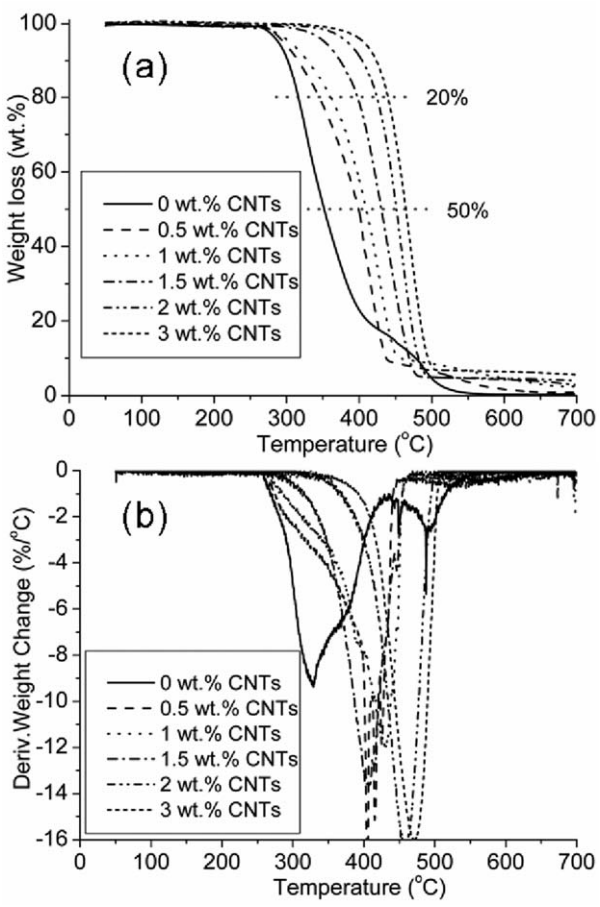

Figure 7. (a) TGA and (b) differential TGA curves of pure SEBS and its composites as a function of CNT content under air condition.

mixing and CNT/SEBS prepared by the EAMM method also indicates that the EAMM method improves effectively the dispersion of CNTs in SEBS matrix, which is consistent with the results of SEM and TEM observations.

Thermal Decomposition of the CNT/SEBS Composites

Figure 7 shows the TGA and differential TGA curves of the samples under air condition. The thermal decomposition of pure SEBS with maximum mass loss rate appears at 328°C and almost no residue remains at 650°C. Compared with the pure SEBS, the temperatures of decomposition with maximum mass loss rate and the residues of the CNT/SEBS composites are evidently improved. In addition, the temperatures of 20% weight loss of the CNT/SEBS composites with 0.5, 1.5, and 3 wt % CNTs are improved from 316.2°C of pure SEBS to 344.5°C, 397.5°C, and 439.5°C, respectively. Meanwhile, the temperatures of 50% weight loss of the CNT/SEBS composites with 0.5, 1.5, and 3 wt % CNTs are improved from 351.8°C of pure SEBS to 399.2°C, 428.6°C, and 463.3°C, respectively. According to the reports,[16,32] a continuous network structured protective layer formed by CNTs is critical for the improved thermal stability, because the network layer acts as a heat shield from energy feedback. The improved thermal stability, as a result of the uniform dispersion of CNTs, also confirms the uniform dispersion of CNTs in SEBS matrix.

CONCLUSIONS

The MWCNT/SEBS composites were prepared by the EAMM method. The efficient embedding of MWCNTs on the surfaces of SEBS particles with the help of electrostatic adsorption was preserved and improved during the subsequential process of melt mixing. Therefore, the dispersion of CNTs in SEBS matrix was improved compared with the CNT/SEBS composites prepared by the conventional melt mixing and a low percolation threshold was achieved at the CNT concentration of 0.186 vol %. Meanwhile, the electrical, mechanical properties, and thermal stability of the CNT/SEBS composites were improved significantly. Importantly, this simple and low-cost method shows the potential for the preparation of CNT/polymer composite materials with enhanced electrical, mechanical properties, and thermal stability for industrial applications.

ACKNOWLEDGMENTS

The authors are grateful to the supports of National Natural Science Foundation of China (No. 51103160). All listed authors take part in the research design, interpretation of data, drafting the paper and approval of the submitted and final versions.

REFERENCES

1. Baughman, R. H.; Zakhidov, A. A.; de Heer, W. A. *Science* **2002**, *297*, 787.
2. Cao, J.; Wang, Q.; Rolandi, M.; Dai, H. *Phys. Rev. Lett.* **2004**, *93*, 216.
3. Spitalsky, Z.; Tasis, D.; Papagelis, K.; Galiotis, C. *Prog. Polym. Sci.* **2010**, *35*, 357.
4. Coleman, J. N.; Khan, U.; Blau, W. J.; Gun'ko, Y. K. *Carbon* **2006**, *44*, 1624.
5. McNally, T.; Potschke, P.; Halley, P.; Murphy, M.; Martin, D. *Polymer* **2005**, *46*, 8222.
6. Kim, Y. J.; Shin, T. S.; Choi, H. D.; Kwon, J. H.; Chung, Y. C.; Yoon, H. G. *Carbon* **2005**, *43*, 23.
7. Zhang, C.; Zhu, J.; Ouyang, M.; Ma, C.; Sumita, M. *J. Appl. Polym. Sci.* **2009**, *114*, 1405.
8. Liu, Q. M.; Tu, J. C.; Wang, X.; Yu, W. X.; Zheng, W. T.; Zhao, Z. D. *Carbon* **2012**, *50*, 339.
9. Andrews, R.; Jacques. D.; Minot, M.; Rantell, T. *Macromol. Mater. Eng.* **2002**, *287*, 395.
10. Potschke, P.; Fornes, T. D.; Paul, D. R. *Polymer* **2002**, *43*, 3247.
11. Zhang, L. Y.; Wan, C. Y.; Zhang, Y. *Compos. Sci. Technol.* **2009**, *69*, 2212.
12. Zhang, Z. N.; Zhang, J.; Chen, P.; Zhang, B. Q.; He, J. S.; Hu, G. H. *Carbon* **2006**, *44*, 692.
13. Gao, J.; Li, Z.; Meng, Q.; Yang, Q. *Mater. Lett.* **2008**, *62*, 3530.
14. Wang, Z.; Fan, X.; Wang, K.; Deng, H.; Chen, F.; Fu, Q. *Compos. Sci. Technol.* **2011**, *71*, 1397.
15. Zhang, Q. H.; Lippits, D. R.; Rastogi, S. *Macromolecules* **2006**, *39*, 658.
16. Wu, Z.; Wang, H.; Tian, X.; Ding, X.; Xue, M.; Zhou, H.; Zheng, K. *Compos. Sci. Technol.* **2013**, *82*, 8.
17. Lu, K. B.; Grossiord, N.; Koning, C. E.; Miltner, H. E.; Mele, B. V.; Loos, J. *Carbon* **2008**, *41*, 8081.
18. Glor, M. *J. Electrostatics* **2005**, *63*, 447.
19. Hearn, G. L. *IEEE Trans Ind. Appl.* **2001**, *37*, 730.
20. Ajayan, P. M.; Schadler, L. S.; Giannaris, C.; Rubio, A. *Adv. Mater.* **2000**, *12*, 750.
21. Liu, T. X.; Phang, I. Y.; Shen, L.; Chow, S. Y.; Zhang, W. D. *Macromolecules* **2004**, *37*, 7214.
22. Hwang, G. L.; Shieh, Y. T.; Hwang, K. C. *Adv. Funct. Mater.* **2004**, *14*, 487.
23. Potschke, P.; Fornes, T. D.; Paul, D. R. *Polymer* **2002**, *43*, 3247.
24. Kim, J. K.; Jun, D. S.; Kim, J. W. *Polymer* **1993**, *34*, 4613.
25. Kojima, Y.; Usuki, A.; Kawasumi, M.; Okada, A.; Fukushima, Y.; Kurauchi, T.; Kamigaito, O. *J. Mater. Res.***1993**, *8*, 1185.
26. Krishnamoorti, R.; Vaia, R. A.; Giannelis, E. P. *Chem. Mater.* **1996**, *8*, 1728.
27. Lu, H. B.; Nutt, S. *Macromol. Chem. Phys.* **2003**, *204*, 1832.
28. Kirkpatrick, S. *Rev. Mod. Phys.* **1973**, *45*, 574.
29. Clerc, J. P.; Girand, G.; Laugier, J. M.; Luck, J. M. *Adv. Phys.* **1990**, *39*,191.
30. Straley, J. P. *Phys. Rev. B* **1977**, *15*, 5733.
31. Fisch, R.; Harris, A. B. *Phys. Rev. B* **1978**, *18*, 416.
32. Kashiwagt, T.; Du, F. M.; Douglas, J. F.; Winey, K. I.; Harris Jr, R. H.; Shields, J. A. *Nat. Mater.* **2005**, *4*, 928.